RESEARCH ON A FLOW-MODE MAGNETO-RHEOLOGICAL IMPACT DAMPER WITH STROKE-ACTIVATED CAPABILITY

Huu-Quan Nguyen^{©1}, Quoc-Duy Bui^{©1,*}, Duc-Nam Nguyen^{1,*}, Quoc Hung Nguyen^{©2}, Long-Vuong Hoang^{©1}

¹Faculty of Mechanical Engineering, Industrial University of Ho Chi Minh City, Ho Chi Minh City, Vietnam

²Institute of Engineering, HUTECH University, Ho Chi Minh City, Vietnam *E-mails: buiquocduy@iuh.edu.vn, nguyenducnam@iuh.edu.vn

Received: 20 January 2025 / Revised: 23 April 2025 / Accepted: 12 May 2025 Published online: 26 June 2025

Abstract. It is widely recognized that impact is an intricate problem that has challenged scientific scholars for many years. Impacts, such as those occurring in high-speed aircraft landings, vehicle accidents, or machine tool operations, pose substantial hazards to human health and safety, as well as cause damage to the structural durability, integrity and sustainability of various facilities. This paper researches a flow-mode magneto-rheological (MR) impact damper (ID) to reduce the effects of shocks and vibrations during sudden impacts. By applying a magnetic field to the magneto-rheological fluid (MRF) within the damper, the damping properties can be adjusted in real-time. The traditional approaches typically use electric coils to generate the required magnetic field, leading to increased complexity and high costs in structure and control systems. To address this limitation, we replace the coils with multiple permanent magnets distributed along the linear displacement of the damper, enabling the generation of a progressive damping force. Therefore, in addition to a more streamlined design, the new configuration equips the MRID with a stroke-activated capability that aids in creating a soft-landing effect, thereby minimizing harm during collisions. To improve the operational efficiency, performance criteria of the damper, including damping force in off and activated states, dynamic range and installation volume, are considered in a design optimization procedure. Optimal solutions for the proposed MRID are simulated using the finite element method (FEM), followed by a detailed design phase. Subsequent analyses and discussions are conducted to provide guidance for future development.

Keywords: adaptive, flow-mode, impact damper, magneto-rheological, stroke-activated.

1. INTRODUCTION

Soft-landing generally refers to a controlled landing process that minimizes harm to human safety while also preventing damage to the integrity of facilities. In impact scenarios, dampers and springs within suspension systems play a crucial role in reducing vibrations; however, they also serve as intermediaries that transmit collision impulses to the surroundings [1]. This transmitted force is a primary cause of danger to involved personnel and damage to equipment. In fixed damping systems, the damping force depends on velocity. At the moment of impact, due to the high collision velocity, fixed damping may generate a large, uncontrollable transmitted force. In contrast, variable damping systems, such as MRIDs, can offer a controllable damping force tailored to the desired level of force transmissibility [2]. This adaptability enables the creation of a soft-landing effect, providing better protection for both humans and infrastructure throughout the impact event.

In recent years, numerous studies have actively employed MRID technology to absorb impact energy, with the goal of safeguarding individuals and device structures across a range of collision scenarios. Notable examples include MR landing gear dampers in lightweight helicopter landing systems [3], MR energy absorbers for helicopter seat suspension systems [4,5], MR landing gear devices for lunar-planetary landers [6], and MR shock absorbers designed for soft landings during elevator emergency crash scenarios [7]. To diminish impacts during high-speed events and mitigate vibrations at lower speeds, essential state parameters of the controlled object, including speed, displacement, and acceleration of the impact load, serve as crucial input conditions for the controller of MRID systems. Following this, the control system computes the requisite MRID force corresponding to the present state of the controlled object and triggers control mechanisms. Moreover, force sensors are integrated into MRID systems to promptly capture input and output forces, thereby enhancing system control [8,9]. The inherent complexities associated with MRID devices and their control systems can lead to an increase in the system's dimensions, weight, and overall cost. Traditional MRIDs with control systems often lack the necessary reliability for emergency situations like elevator mishaps and vehicle collisions. Consequently, the development of a compact, adaptable MRID with enhanced reliability becomes imperative.

In this study, the authors develop an MRID aimed at mitigating the damage resulting from sudden collisions. The proposed MRID operates based on the flow-mode principle of MRF and is activated by the magnetic fields of permanent magnets. The new approach eliminates the need for coil winding and a control system (including sensors, power supplies, and a control scheme), which are commonly found in traditional MRIDs. This results in a simplified design and, consequently, reduced manufacturing costs. In addition, the proposed MRID can operate independently of external power sources, offering

fail-safe capabilities and high reliability. The permanent magnets are strategically distributed along the damper's length to generate an impact damping force that increases with stroke, thereby providing a soft-landing effect. The study begins with the consideration of a dynamic model for a drop-induced impact, followed by the description of the flow-mode MRID configuration. Subsequently, the MRID is modeled and optimized in terms of geometric structure, with a focus on performance parameters such as expected damping force, dynamic range, and operational space. Based on the optimal results, a detailed design of the optimized MRID is conducted, accompanied by dedicated analyses and discussions.

2. EQUATION OF MOTION AND MODELING OF THE FLOW-MODE MRID

2.1. Equation of motion

The damping force generated by MRID is typically confined within a specific range, determined by the design structure. This restricted range influences the efficiency of MRID. To ensure the device functions effectively, the damping force of the MRID must be suitably tailored for various types of impacts, based on different input excitations. Therefore, it is imperative to optimally design the structure and parameters of MRID, as well as to develop a dynamic model that accurately describes the characteristics of the collision process.

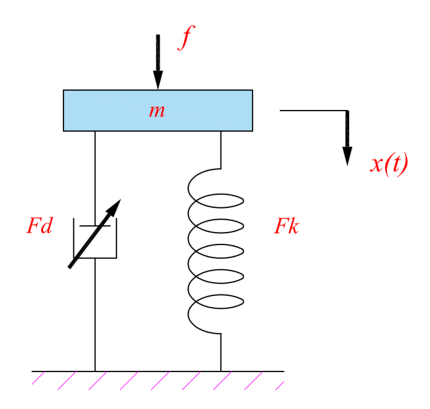


Fig. 1. A single degree of freedom system subjected to an impulse

During the collision process, the system experiences vibrations caused by an impulse excitation. This impulse, acting over a very short period of time, results in a sudden change in the momentum of the system. Firstly, we consider the response of a single degree of freedom system subjected to an impulsive excitation (Fig. 1). The system consists of a spring and an MR damper, firmly affixed to the base below. The equation of motion for the system can be written as follows

$$m\ddot{x} + c\dot{x} + kx = 0. \tag{1}$$

Solution to the equation results in

$$x(t) = e^{-\zeta \omega_n t} \left\{ x_0 \cos \omega_d t + \frac{\dot{x}_0 + \zeta \omega_n x_0}{\omega_d} \sin \omega_d t \right\}. \tag{2}$$

In the above equation, m is the mass of the post-collision system, c and k are the damping coefficient and spring stiffness, respectively. x(t) is the relative displacement of the suspension system caused by the impulse excitation. The damping ratio ζ , natural frequency ω_n , and damped frequency ω_d are given by the following equations

$$\zeta = \frac{c}{2m\omega_n}, \quad \omega_n = \sqrt{\frac{k}{m}}, \quad \omega_d = \omega_n \sqrt{1 - \zeta^2}.$$
 (3)

Assuming the system is initially at rest before the impulse excitation is applied ($x = \dot{x} = 0$ for t < 0 or at $t = 0^-$) and the magnitude of the impulse is f, the initial velocity \dot{x}_0 is determined as f/m. Referring back to Eq. (2), the steady-state response of the system can be inferred as follows

$$x(t) = \frac{f e^{-\zeta \omega_n t}}{m \omega_d} \sin \omega_d t. \tag{4}$$

In this research, the design of the MRID is based on the quasi-static model approach. The behavior of the MRID can be regarded as similar to that of a dry friction damper. Therefore, by using an equivalent damping coefficient c_{eq} , such that the work done per half-cycle due to this coefficient equals the work produced by the MRID damping force, as in [10], we have

$$W_d = \int_{\theta}^{\pi/\omega_d} F_{eq} \dot{x}(t) dt = \int_{\theta}^{\pi/\omega_d} c_{eq} \dot{x}^2(t) dt = 2 |F_{rd}| X.$$
 (5)

In the above, X denotes the magnitude of the system's vibration, while F_{rd} represents the required damping force of the system. By substituting $c_{eq} = 2m\omega_n\zeta$ from Eq. (3) and the first-order derivative of Eq. (4) into Eq. (5), F_{rd} is determined by

$$F_{rd} = \frac{f^2 c_{eq} (e^{-2\pi \zeta \omega_n / \omega_d} - 1)}{8X \zeta m^2 \omega_n} = \frac{f^2 (e^{-2\pi \zeta \omega_n / \omega_d} - 1)}{4Xm}.$$
 (6)

Based on the performance index ITAE (Integral of Time multiplied by Absolute Error) [11], the damping ratio for the second-order oscillatory system is selected as 0.7 to ensure an appropriate response of the suspension system to the impact.

2.2. Modeling of the flow-mode MRID

The proposed configuration of the flow-mode MRID featuring permanent magnets with stroke-activated capability is illustrated in Fig. 2. The damper comprises two main components: a cylinder and a piston assembly unit. The cylinder serves as the outer housing, guiding and securing the piston while enclosing the MRF. The piston assembly unit (referred to as "piston" hereafter) consists of the piston rod, piston core, and piston guides, combined into a valve-like structure.

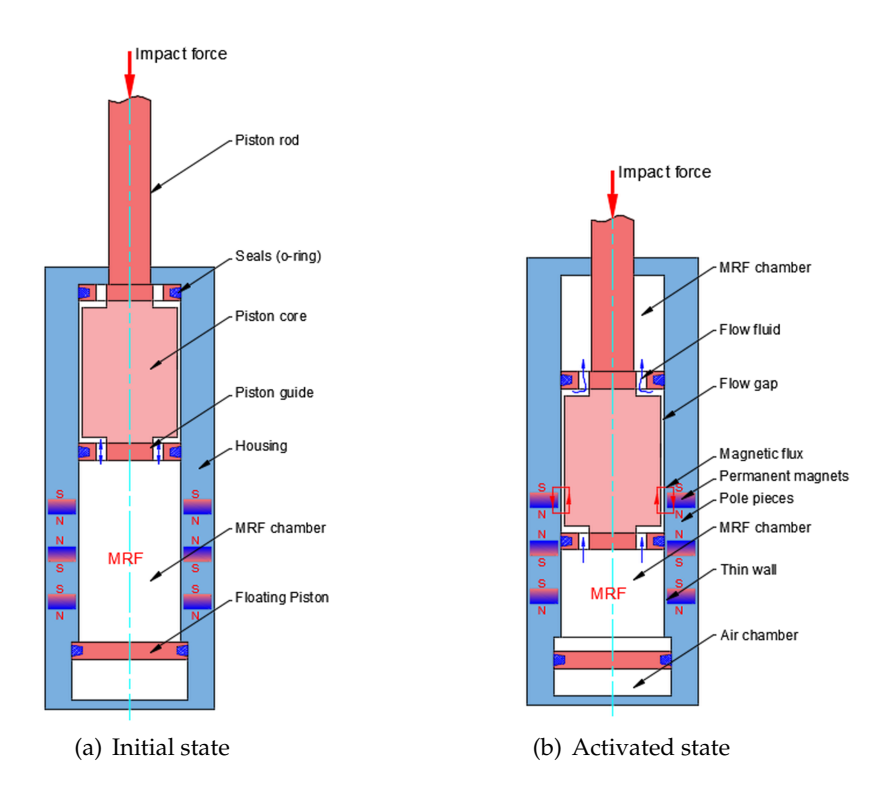


Fig. 2. Configurations of the MRIDs

The MRF is distributed and fully contained within the upper and lower chambers, enabling movement through orifices in the annular duct as the piston shifts position. The ring-shaped permanent magnets are arranged in opposite pole directions and interspersed with magnetic pole pieces. They are positioned within the cylinder from the midpoint to the stroke's end. Additionally, the MRID incorporates a gas chamber isolated from the MRF chambers by a floating piston, which functions as an accumulator, ensuring effective communication of the MRF.

In the initial state, the piston core resides beyond the magnetic field region of the permanent magnets, resulting in an open electromagnetic circuit. Upon exposure to the impulse, the MRID undergoes downward movement of the piston towards the floating piston, as illustrated in Fig. 2. Subsequently, the MRF in the lower chamber flows upward through the annular duct. At this point, the piston core enters the effective region of the magnets, closing the electromagnetic circuit. This action initiates the generation of a magnetic field that passes across the MRF gap, thereby producing additional damping force. The further the piston moves towards the end of the stroke, the more MRF is activated, leading to a greater generated damping force. As a result, a soft-landing effect is guaranteed, and the proposed flow-mode MRID can be activated according to its

stroke without any control. This mechanism prevents the MRID from producing a sudden high-resistance force that could result in injury to humans or damage to the device's mechanical structure. Furthermore, the number of permanent magnets and their distribution can be adjusted intentionally for specific impact damping performance objectives.

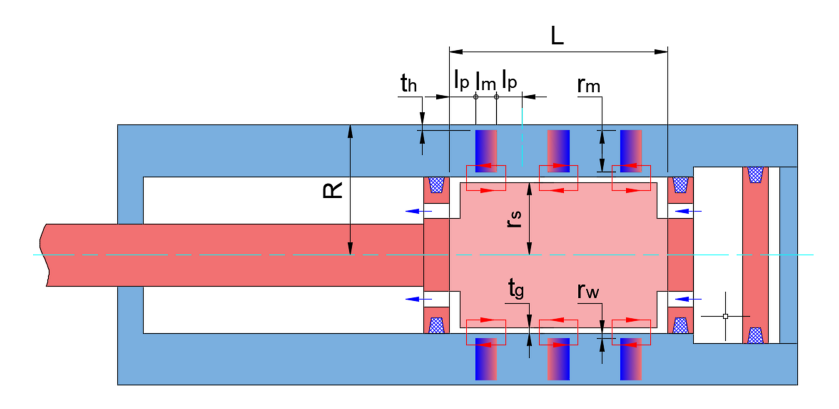


Fig. 3. Geometry of the MRIDs (fully activated state)

The structural geometry of the proposed flow-mode MRID is depicted in Fig. 3. Assuming a quasi-static behavior and a linear velocity profile of the MRF in the annular duct, the damping force F_d is determined according to the formula

$$F_d = F_0 + F_{\tau}. \tag{7}$$

In the above equation, F_0 is the off-state force, F_{τ} is the damping force caused by the MRF yield stress. The off-state force comprises the bias damping force due to the pressure in the accumulator F_{Bias} , the viscous damping force F_{η} , and the Coulomb friction force between the piston and the O-rings, represented as follows

$$F_0 = F_{Bias} + F_{\eta} + F_{or}. \tag{8}$$

The bias damping force F_{Bias} is calculated by the following equation

$$F_{Bias} = A_s P_0 \left(\frac{V_0}{V_0 + A_s x}\right)^{\alpha},\tag{9}$$

where A_s is the cross-sectional area of the piston shaft, x is the displacement of the piston, α is the coefficient of thermal expansion, P_0 and V_0 are the initial pressure and volume of the gas chamber, respectively. Considering L as the operating length of the MRF in the duct, A_p as the cross-sectional area of the piston core, v as the velocity of the piston, η as the post-yield viscosity of the MRF, r_g and t_g as the average radius and thickness of the MRF gap, respectively, the viscous damping force F_{η} is calculated using the formula

$$F_{\eta} = \frac{6\eta L}{\pi r_g t_g^3} (A_p - A_s)^2 \dot{x}. \tag{10}$$

The damping force caused by the MRF yield stress F_{τ} is the controllable dominant component of the damping force F_d . Neglecting minor losses of the MRF flow in the duct, F_{τ} can be determined in the form of:

$$F_{\tau} = \frac{2c_p l_p \tau_y}{t_s} \left(A_p - A_s \right), \tag{11}$$

where τ_y is the yield stress of the MRF, l_p is the length of each magnetic pole segment, and c_p is the coefficient characterizing the MRF flow profile [12].

In this study, the MRF type 132-DG manufactured by Lord Corporation was used to model the proposed MRID. The yield stress τ_y dependent on the magnetic field H is calculated by the formula

$$\tau_{\nu} = 2.717 * 10^{5} C\Phi^{1.5329} \tanh(6.33 \times 10^{-6} H), \tag{12}$$

where C is the medium fluid coefficient set to 1, Φ represents the volume fraction of iron set to 0.32. To solve the electromagnetic circuit, the finite element method (FEM) is employed. This method leverages the computational power of modern computers while providing a significantly precise solution, as it considers both a large number of magnetic flux links and the non-uniform distribution of magnetic density throughout the MRF duct length. The finite element model of the proposed MRID structure is constructed using the 2D axisymmetric element (PLANE 233) in the ANSYS software.

3. CONSTRAINED OPTIMIZATION PROBLEM FORMULATION

In this paper, the Adaptive Multiple-Objective Optimization (AMO) method is applied to address the MRID design problem. AMO is a multi-objective optimization technique that combines the Kriging response surface algorithm and the direct optimization Multiple-Objective Genetic Algorithm (MOGA). This method follows a similar approach to MOGA but with a focus on time efficiency. Notably, the optimization process does not assess all design points. By using a Kriging error predictor, the necessary number of evaluations for finding solutions on the first Pareto front is reduced. AMO, with the Kriging response surface algorithm, can refine continuous input parameters, including those with potential usability. By generating and adding refined points within regions of the response surface, it enhances areas where such refinement is most crucial. The integration of the Kriging model into the MOGA framework offers key advantages by significantly improving computational efficiency and enabling intelligent guidance through the design space. It not only reduces the reliance on costly full evaluations but also identifies regions of high uncertainty for targeted refinement, thereby ensuring a more comprehensive and effective exploration of optimal design solutions. Fig. 4 illustrates the workflow of the AMO optimization method. Reference [13] provides more detailed and comprehensive information.

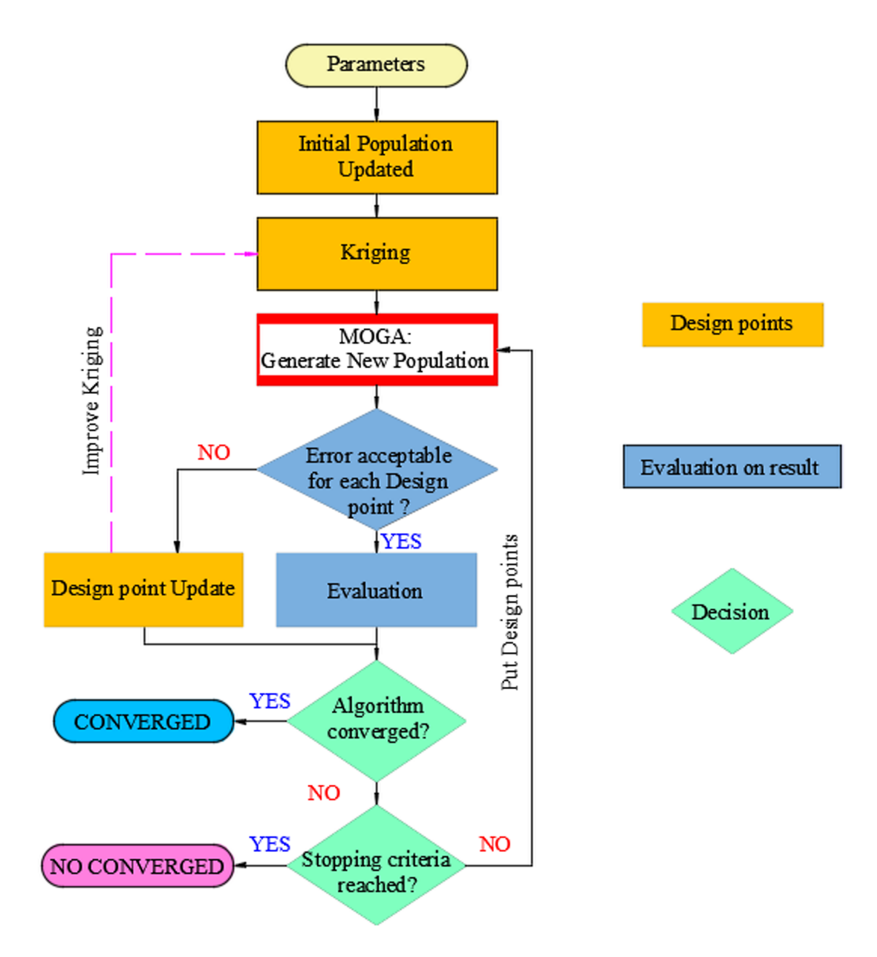


Fig. 4. Workflow of AMO

In this design scenario, the piston core and housing are made of magnetic material C45 steel, while the piston shaft, piston guides and floating piston are made of non-magnetic material. The ring-shaped permanent magnets are composed of NdFeB material, grade N35. The MRF in the chambers is sealed with 70-durometer NBR rubber O-rings, compressed at a rate of 15%. The gas chamber, separated by the floating piston, contains Nitrogen gas, known for its chemical inertness under normal conditions.

The proposed flow-mode MRID is designed for an impact damping system, assuming a mass of 20 kg free-dropping from a height of 1 m. Given that after impact, the dropping object adheres to and moves together with the suspension system. The spring stiffness is set at 14 kN/m. Using the equation of motion (4), the displacement amplitude of the piston is calculated to be 0.07 m, with an average velocity of 2.15 m/s. In this case, the required damping force for the system, as determined from Eq. (6), is 1117 N. This is also the expected damping force value F_e for the design optimization problem. Upon

impact, the piston sequentially passes through each permanent magnet, progressively closing the magnetic circuit and gradually activating the yield stress damping force of the proposed MRID. The design objective is to ensure that the required damping force is achieved, allowing the MRID to stop at the end of its working stroke while providing an effective soft-landing.

In order to facilitate installation in confined workspaces, the operating length of the MRF in the duct L and the radius of the piston R are limited to 40 mm and 25 mm, respectively. To enhance compatibility with various impact scenarios, the MRID is expected to have a high dynamic range D_r , defined by the ratio of the damping force F_d and off-state force F_0 . This design feature also allows the MRID to generate the necessary maximum damping force during impacts without causing sudden resistance forces that might affect individuals or the device structure.

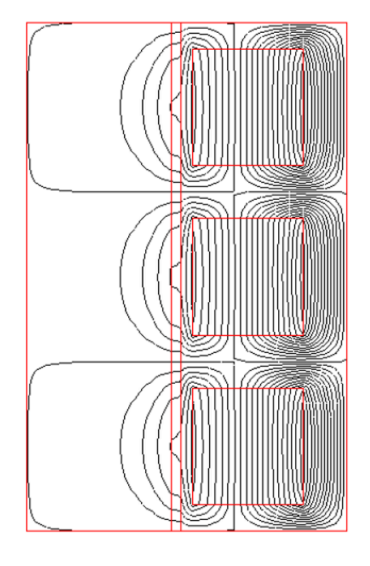
Considering the above, the optimization problem for the proposed flow-mode MRID can be stated as follows: Determine the optimal geometric parameters of the MRID to maximize the dynamic range D_r , subject to the maximum damping force F_d being greater than the expected damping force value F_e .

4. RESULTS AND DISCUSSIONS

Based on the modeling and optimization outlined above, this section presents the optimal solutions for the proposed flow-mode MRID design. The magnetic flux lines and magnetic flux density for the optimized MRID with stroke-activated capability are showcased in Figs. 5 and 6, respectively.

As the MRID experiences the impulse, the piston core gradually enters the operating region of each magnet, successively closing the electromagnetic circuits, as shown in Fig. 5. Consequently, the MRID progressively attains its peak damping force. In Fig. 6, it is noticeable that the flux passing through the thin section between the magnets and the MRF gap almost reaches saturation. The magnetic flux is then directed through the MRF gap and distributed along the entire length of the magnetic pole pieces.

Through the optimization process, the performance parameters of the MRID undergo significant enhancements. The device now achieves the desired objectives of a wide dynamic range of 32.45 and a maximum damping force of 1198.5 N, greater than the expected damping force of 1117 N. This results in an optimal design, where the proposed MRID can flexibly address diverse impact scenarios, exhibiting a low off-state force of 36.8 N, thereby diminishing abrupt resistance forces on individuals and the device structure. Additionally, the device is characterized by its compactness, lightness, safety, and effectiveness for an impact damping system. The optimal solutions using the AMO optimization algorithm for the proposed flow-mode MRID are detailed in Table 1.



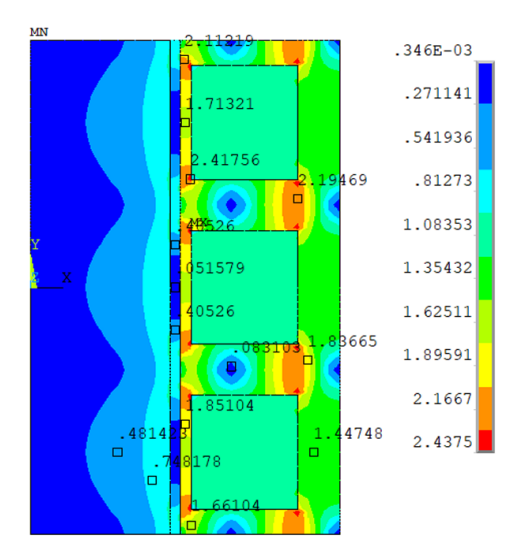


Fig. 5. Magnetic flux lines of the MRID

Fig. 6. Magnetic flux density of the MRID

Table 1. Optimal solutions of the proposed MRID

Parameters (mm)	Bounds		- Optimal values
	Lower	Upper	Optimal values
MRF duct length L	_	40	40
PM height l_m	5	15	9.17
Magnetic pole length l_p	_	_	2.08
MRD radius R	_	25	25
PM width t_m	4	10	8.57
Shaft radius r_s	8	16	11.27
MRF gap thickness t_g	0.8	1.6	0.81
Thin wall thickness r_w	0.8	1.2	0.92
Housing thickness t_h	_	_	3.43
Max. damping force F_d (N)	_	_	1198.5
Off-state force (N)	_	_	36.8
Dynamic range	_	_	32.45

The results also indicate that in order to achieve the necessary damping force, the thickness of the MRF gap t_g and the thickness of the thin section r_w tend to decrease towards their lower bounds. This trend is consistent with some previous studies [14,15]. Nevertheless, it is essential to maintain these dimensions above 0.8 mm to ensure the MRF can effectively transition between chambers and to uphold the manufacturability of the thin section. On the other hand, while reducing the shaft radius r_s may offer beneficial outcomes, this approach is constrained by the structural integrity of the device.

Based on the optimal results outlined above, a 3D design model of the optimized MRID is developed for subsequent research in the upcoming phase, as depicted in Fig. 7.

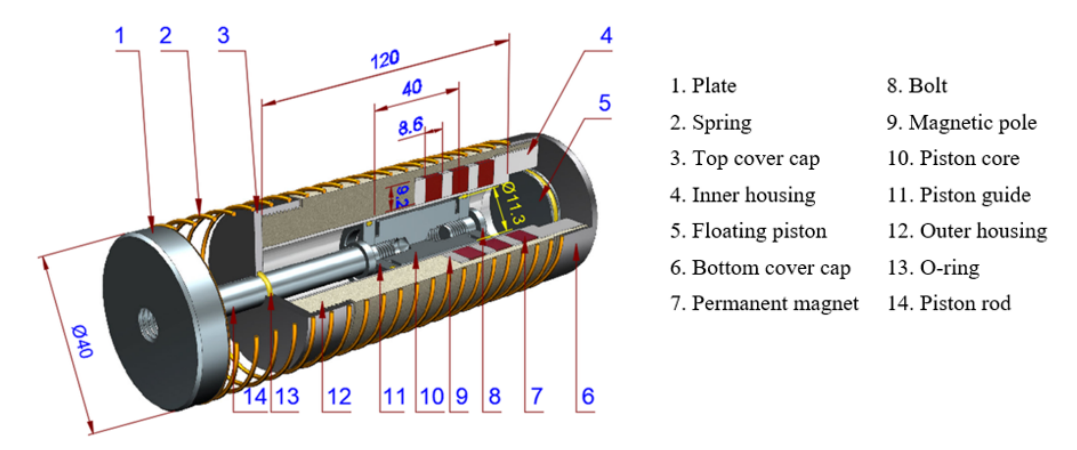


Fig. 7. Quarter-section 3D view of the optimized flow-mode MRID

5. CONCLUSIONS

In this study, a flow-mode MRID incorporating permanent magnets, designed to self-actuate based on the working stroke without requiring a control system, was proposed for impact damping applications. Contrasted with traditional flow-mode MRIDs, this new damper has a simple structure without any magnetic coils, thus eliminating the need for intricate control mechanisms, thereby enhancing reliability. Moreover, these advantages facilitate manufacturing and maintenance, leading to substantial reductions in production costs and enhancing commercial competitiveness. Based on the quasi-static model, the AMO optimization process using FEM was conducted for the basic geometric parameters of the damper. The optimal results facilitate enhancements in the MRID's performance characteristics, including dynamic range and damping force. Additionally, the study suggests that configurations incorporating multiple magnets or coils can yield heightened damping forces, meeting the requirements for high-load applications. However, when transferring the proposed MRID design from simulation to actual production and system implementation, several practical issues may arise. First, environmental factors such as temperature and contamination can alter MRF behavior, impacting damping consistency. Second, changes in the mechanical properties of MRF during extended periods of inactivity must also be considered. Lastly, regulatory standards, safety testing, and scalability for mass production must be addressed to ensure commercial viability and compliance. In the subsequent research phase, the proposed flow-mode MRID with stroke-activated capability will undergo prototyping, testing, and comprehensive evaluation to validate its functionality further. Moreover, modern modeling and optimization

tools such as NURBS-based isogeometric analysis, NURBS response surface, and balancing composite motion optimization [16, 17] will be considered to improve solution accuracy.

DECLARATION OF COMPETING INTEREST

The authors declare that they have no known competing financial interests or personal relationships that could have appeared to influence the work reported in this paper.

ACKNOWLEDGMENT

This research is funded by Vietnam National Foundation for Science and Technology Development (NAFOSTED) under grant number 107.03-2023.86.

REFERENCES

- [1] Q. H. Nguyen, S. B. Choi, and J. K. Woo. Optimal design of magnetorheological fluid-based dampers for front-loaded washing machines. *Proceedings of the Institution of Mechanical Engineers, Part C: Journal of Mechanical Engineering Science*, **228**, (2013), pp. 294–306. https://doi.org/10.1177/0954406213485908.
- [2] S. Jin, L. Deng, J. Yang, S. Sun, D. Ning, Z. Li, H. Du, and W. H. Li. A smart passive MR damper with a hybrid powering system for impact mitigation: An experimental study. *Journal of Intelligent Material Systems and Structures*, **32**, (2021), pp. 1452–1461. https://doi.org/10.1177/1045389x20988085.
- [3] Y.-T. Choi, R. Robinson, W. Hu, N. M. Wereley, T. S. Birchette, A. O. Bolukbasi, and J. Woodhouse. Analysis and control of a magnetorheological landing gear system for a helicopter. *Journal of the American Helicopter Society*, **61**, (2016), pp. 1–8. https://doi.org/10.4050/jahs.61.032006.
- [4] Z. Feng, Z. Chen, and X. Xing. An adaptive shock mitigation control method for helicopter seat system with magnetorheological energy absorbers. *Journal of Intelligent Material Systems and Structures*, **33**, (2021), pp. 987–1001. https://doi.org/10.1177/1045389x211038708.
- [5] M. Wang, Z. Chen, and N. M. Wereley. Adaptive magnetorheological energy absorber control method for drop-induced shock mitigation. *Journal of Intelligent Material Systems and Structures*, **32**, (2020), pp. 449–461. https://doi.org/10.1177/1045389x20957100.
- [6] T. Maeda, M. Otsuki, and T. Hashimoto. Protection against overturning of a lunar-planetary lander using a controlled landing gear. *Proceedings of the Institution of Mechanical Engineers, Part G: Journal of Aerospace Engineering*, **233**, (2017), pp. 438–456. https://doi.org/10.1177/0954410017742931.
- [7] J. Zheng, J. Zhao, L. Wang, Z. Li, W. Dong, and E. Shiju. Optimal control for soft-landing in elevator emergency crash using multiple magnetorheological shock absorbers. *Journal of Intelligent Material Systems and Structures*, **33**, (2022), pp. 2454–2469. https://doi.org/10.1177/1045389x221085646.
- [8] M. Jiang, X. Rui, W. Zhu, F. Yang, and Y. Zhang. Design and control of helicopter main reducer vibration isolation platform with magnetorheological dampers. *International Journal*

- of Mechanics and Materials in Design, 17, (2021), pp. 345–366. https://doi.org/10.1007/s10999-021-09529-x.
- [9] Y. T. Choi, N. M. Wereley, and G. J. Hiemenz. Three-axis vibration isolation of a full-scale magnetorheological seat suspension. *Micromachines*, **15**, (2024). https://doi.org/10.3390/mi15121417.
- [10] C. W. de Silva. *Vibration: fundamentals and practice*. CRC Press, (1999). https://doi.org/10.1201/noe0849318085.
- [11] R. C. Dorf and R. H. Bishop. *Modern control systems*. Pearson Education Inc., (2011).
- [12] J. D. Carlson, D. M. Catanzarite, and K. A. St. Clair. Commercial magneto-rheological fluid devices. *International Journal of Modern Physics B*, **10**, (1996), pp. 2857–2865. https://doi.org/10.1142/s0217979296001306.
- [13] ANSYS Inc. DesignXplorer user's guide. Canonsburg, PA, (2021).
- [14] Q.-D. Bui, L.-V. Hoang, H.-Q. Nguyen, and Q. H. Nguyen. Design and experimental evaluation of a novel flow-mode magnetorheological damper without accumulator. *Journal of Intelligent Material Systems and Structures*, **35**, (2024), pp. 1291–1303. https://doi.org/10.1177/1045389x241256094.
- [15] H.-Q. Nguyen, Q. H. Nguyen, Q.-D. Bui, and D.-N. Nguyen. Optimal design of a magnetorheological damper for above-knee prosthetic leg. In *Proceedings of the International Conference on Sustainable Energy Technologies (ICSET 2023), Green Energy and Technology*, Springer Nature Singapore, (2024), pp. 369–378. https://doi.org/10.1007/978-981-97-1868-9_38.
- [16] L. B. Nguyen, C. H. Thai, N. T. Dang, and H. Nguyen-Xuan. Transient analysis of laminated composite plates using NURBS-based isogeometric analysis. *Vietnam Journal of Mechanics*, **36**, (2014), pp. 267–281. https://doi.org/10.15625/0866-7136/36/4/4129.
- [17] T. Le-Duc, Q.-H. Nguyen, and H. Nguyen-Xuan. Balancing composite motion optimization. *Information Sciences*, **520**, (2020), pp. 250–270. https://doi.org/10.1016/j.ins.2020.02.013.